Rational G^2 Splines

Kęstutis Karčiauskas and Jörg Peters

March 28, 2011

Abstract

We develop a class of rational, G^2-connected splines of degree 3 that allow modeling multiple basic shapes, such as segments of conics and circle arcs in particular, in one structure. This can be used, for example, to have portions of a control polygon exactly reproduce segments of the shapes while other portions blend between these primary shapes. We also show how to reparameterize the splines to obtain parametrically C^2 transitions.

1 Introduction

In conceptual design one may view an outer surface as derived from primary surfaces that represent functionality or simplicity of shape, for example quadrics and cyclides. Extending this way of thinking to implementation, however, creates challenges. When the pieces are created in isolation, as separate entities, they must be combined using intersections, fillets and blends. It is therefore useful to have an underlying structure, not necessarily exposed to the designer, that supports the conceptual design but avoids the *a posteriori* need for stitching the conceptual pieces together. Such built-in blending is also useful when varying designs while preserving constraints as part of a shape optimization process.

While these challenges are more apparent in the surface case, they can already be studied in the curve case. If the primary shapes are polynomial rather than rational, linearly combining B-splines provides a well-known solution: for many applications, C^2 cubics provide sufficient smoothness and flexibility with low degree. Often, however, non-polynomial shapes, conics in particular, have to be reproduced exactly, for example to model the action of a machine tool or to support differential equation based on the variation of the normal or curvature. There

are two known approaches. The first, modeling conics as projections of C^2 curves in homogeneous space leads to high degree parameterizations, e.g. already degree 6 to reproduce a circle [BP97]. The second, at the opposite end of the spectrum, is to use rational quadratic pieces in Bernstein-Bézier form (BB-form) to exactly represent *individual* conic shapes; but this lacks built-in smooth transitions.

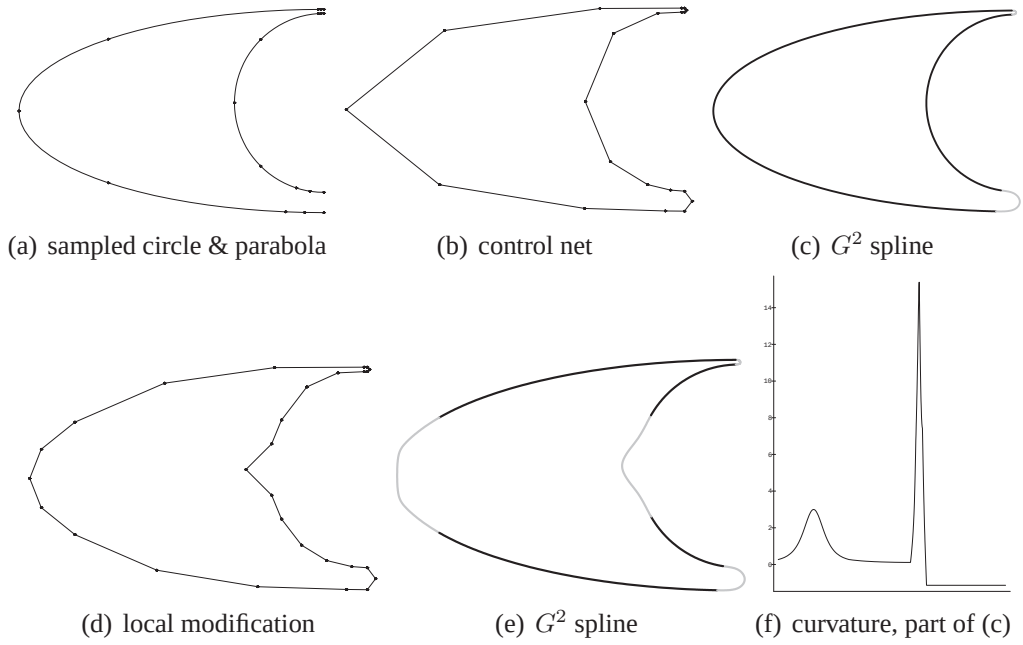

(a) sampled circle & parabola (b) control net (c) G^2 spline

(d) local modification (e) G^2 spline (f) curvature, part of (c)

Figure 1: Exact reconstruction of conic pieces and localized blending.

This paper develops an analogue of the polynomial C^2 cubic B-spline paradigm that can include a sequence of approximate or exact rational primary shapes, such as segments of conics or rational spirals, and automatically combine them into a smooth whole. In place of a non-uniform knot sequence, we employ geometrically smooth transitions between the polynomial pieces. In particular, our rational cubic spline curves will be G^2 continuous at the knot positions. Fig. 1 shows one design scenario: connecting a parabola to an inserted circular arc. In (a) the parabola and half of a circle are sampled non-uniformly (small dots) in anticipation of subsequent blending, i.e. more densely near the end points. The proposed algorithm automatically generates the spline control polygon (b) from these samples so that the arcs are exactly reproduced. The remaining, user-set or auto-generated control points outline a smooth blend. The resulting rational G^2 spline is shown in (c): The thick segments are on the original primitives, the thinner grey ones form

a smooth transition. Subfigure (f) shows the curvature of $2/3$ of this periodic spline, excluding the high-curvature segment, *top right* in (c), since its curvature dwarfs the rest of the graph. Note the horizontal section on the *right* of the graph in (c), validating exact reproduction of the circle segment. The control net can be refined repeatedly and locally for additional design changes. In (d) four vertices are inserted in each of the parabola and the circle piece. The points are not perturbed away from the parabola's, but rather a geometric continuity constant β_i is changed resulting in a flattened left segment. In (e), the preserved curve segments are rendered thick.

Fig. 2 shows a second scenario: reproducing an existing simple design curve, here a circle, and locally modifying it while leaving the remaining circle segments in place. The shape in (c) is represented as a single rational G^2 spline curve of degree 3.

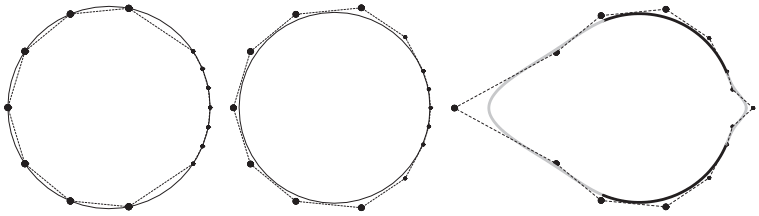

(a) circle sampled (b) control polygon and G^2 spline (c) local adjustment

Figure 2: **Non-uniform spacing for local adjustment.** (a) A designer places points non-uniformly on the circle to initiate local adjustments. Small disks correspond to an opening angle of $\pi/16$, large ones to $3\pi/16$. (b) The derived control net and the exact circle generated by the G^2 spline. (c) Local modification. Thick segments lie exactly on the circle.

Overview. Section 3 reviews geometric continuity. Section 4 defines a rational cubic G^2 spline. Section 5 shows how to include any rational cubic curve piece into the spline, conics in particular. Section 6 compares the rational cubic G^2 spline with two non-stationary subdivision algorithms, [MWW01, Rom09]. Section 7 sketches a subdivision scheme derived from the cubic G^2 spline.

Some applications require not only the shape but also its parametric traversal to be smooth. Therefore Section 8 proposes a rational quadratic reparameterization of the Hermite-expansions of the rational G^2 cubics in order to exactly model conics, but with pieces that join parametrically C^2 rather than G^2. Section 9

proposes a rational cubic reparameterization that allows recovering, as a special uniform case, the projection-based splines of degree 6 proposed by [BP97]. This construction yields C^2 continuity in homogeneous space. Section 10 briefly discusses basis functions and extensions.

Since the presented construction of rational G^2 splines yields a superset of C^2 splines, capable both of modeling non-uniform parameterization and reproduction of rational curve segments, it is not surprising that individual formulas are more complex. The simple underlying combinatorial structure of classical splines, though, is preserved. In full generality, the derivations are best done with the help of a symbolic computation system, rather than written out in detail. But the resulting formulas are displayed in full detail and generality so that a reader may verify or apply them directly in implementations.

2 Literature

We do not attempt to survey the extensive literature on piecewise polynomial, trigonometric and subdivision curve constructions, but survey the foundations of reproducing conic sections. Section 6 compares G^2 splines to two pertinent newer constructions, [MWW01, Rom09] representative of approaches like [ADS10]. The classical literature defines rational constructions [Boe87, Far06] capable of reproducing individual conics. Moreover, splines provide built-in continuity. But standard parametric C^2 continuity in homogeneous space leads to high degree [BP97]. Instead, we leverage geometric continuity [MB89, Joe90]. In particular, our approach to defining a new class of cubic G^2 splines is based on mimicking splines with *non-uniform* knots, namely by G^2 splines with geometric continuity. The underlying combination of rational constructions and geometric continuity has in principle been discussed in [GB88, HB89, MB91]; but the general theory has not been leveraged for specific reproducing constructions of the type we present in this paper. Therefore, we review the pertinent parts of the theory next.

3 Geometric continuity

While non-uniform knot spacing is an important feature of B-spline functions, for geometric constructions, and especially of rational curves, it is simpler to use local coordinates. That is we model non-uniformity by joining curve segments in Bernstein-Bézier form with geometric continuity. A rational curve f of degree n

is in Bernstein-Bézier form (BB-form) if

$$f := \frac{\sum_{k=0}^{n} w_k \mathbf{b}_k B_k^n(u)}{\sum_{k=0}^{n} w_k B_k^n(u)} \qquad B_k^n(u) := \binom{n}{k}(1-u)^{n-k}u^k. \tag{1}$$

Here $\mathbf{b}_k$ are the affine BB-coefficients. Geometric continuity is defined next.

Definition 1 (G^2 continuity) *Given a map f defined over the interval $[a, b]$ and a map g over $[c, d]$ so that $f(b) = g(c)$, f and g join G^1 at the common point if for some scalar $\beta > 0$*

$$g'(c) = \beta f'(b), \tag{2}$$

and G^2 if additionally there exists $\gamma \in \mathbb{R}$,

$$g''(c) = \beta^2 f''(b) + \gamma f'(b)\ . \tag{3}$$

In the above definition, we can linearly reparameterize the domains of f and g. If we define

$$\tilde{f} := f(k_0 u + a), \quad \tilde{g} := g(k_1 u + c), \quad k_0 := b - a, k_1 := d - c, \tag{4}$$

then $\tilde{f}$ and $\tilde{g}$ are each parameterized over $[0, 1]$ and (2) and (3) become

$$\tilde{g}' = \tilde{\beta}\tilde{f}'\ , \quad \tilde{g}'' = \tilde{\beta}^2\tilde{f}'' + \tilde{\gamma}\tilde{f}'\ ; \quad \tilde{\beta} := \frac{k_1}{k_0}\beta\ ,\ \tilde{\gamma} := \frac{k_1^2}{k_0}\gamma\ . \tag{5}$$

For example, if f and g are consecutive pieces of a C^2 spline and Δ_f and Δ_g are the lengths of their knot-intervals then reparameterization as in (4) yields $\tilde{\beta} = \frac{\Delta_g}{\Delta_f}$ and $\tilde{\gamma} = 0$ in (5). Hence, we say that two abutting curve segments $\tilde{f}$ and $\tilde{g}$, parameterized over the unit interval and with derivatives related by $\tilde{\beta} = \frac{\Delta_g}{\Delta_f}$ and $\tilde{\gamma} = 0$, join *parametrically C^2*; and if $\tilde{\beta} = 1$ for all joins, they join *uniformly*.

If, for the unit-interval parametrized pieces $\tilde{f}$ and $\tilde{g}$, we reverse the parameterization to $\breve{f}(u) := \tilde{f}(1-u)$, $\breve{g}(u) := \tilde{g}(1-u)$ then

$$\breve{f}'(0) = \breve{\beta}\breve{g}'(1),\ \breve{f}''(0) = \breve{\beta}^2\breve{g}''(1) + \breve{\gamma}\breve{g}'(1)\ , \qquad \breve{\beta} := \frac{1}{\beta}\ ,\ \breve{\gamma} := \frac{\gamma}{\beta^3}\ . \tag{6}$$

And if the curve pieces $\hat{f}(u) := \tilde{f}(e(1-u)+u)$ and $\hat{g}(u) := \tilde{g}(\bar{e}u)$ split a G^2 spline then

$$\hat{g}'(0) = \hat{\beta}\hat{f}'(1),\ \hat{g}''(0) = \hat{\beta}^2\hat{f}''(1) + \hat{\gamma}\hat{f}'(1)\ ; \tag{7}$$

$$\hat{\beta} := \frac{\bar{e}}{1-e}\beta\ ,\ \hat{\gamma} := \frac{\bar{e}^2}{1-e}\gamma\ .$$

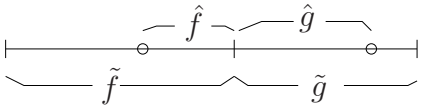

By equating the derivatives up to second order, we obtain the following constraints on the BB-coefficients for G^2 continuity.

Lemma 1 (Local G^2 join) *Let f and $\tilde{f}$ be rational curve segments of degree n in BB-form (Bernstein-Bézier form)*

$$f := \frac{\sum_{k=0}^n w_k \mathbf{b}_k B_k^n(u)}{\sum_{k=0}^n w_k B_k^n(u)} \qquad \tilde{f} := \frac{\sum_{k=0}^n \tilde{w}_k \tilde{\mathbf{b}}_k B_k^n(u)}{\sum_{k=0}^n \tilde{w}_k B_k^n(u)}.$$

Then $\tilde{f}$ and f join *G^2, i.e. $\tilde{f}'(0) = \beta f'(1)$ and $\tilde{f}''(0) = \beta^2 f''(1) + \gamma f'(1)$, if $w_n := \tilde{w}_0$ and the BB-coefficients satisfy $\mathbf{b}_n := \tilde{\mathbf{b}}_0$ and*

$$\mathbf{b}_{n-1} := a_0\mathbf{b}_{n-2} + a_1\mathbf{b}_n + a_2\tilde{\mathbf{b}}_2\ , \quad \tilde{\mathbf{b}}_1 := \tilde{a}_0\mathbf{b}_{n-2} + \tilde{a}_1\mathbf{b}_n + \tilde{a}_2\tilde{\mathbf{b}}_2, \tag{8}$$

where

$$\begin{aligned} den &:= w_{n-1}\big(w_n\gamma + 2(n\tilde{w}_1 - w_n)\beta + 2(nw_{n-1} - w_n)\beta^2\big)\ , \\ a_0 &:= \frac{(n-1)w_{n-2}w_n\beta^2}{den}\ , a_2 := -\frac{(n-1)\tilde{w}_2 w_n}{den}\ , a_1 := 1 - a_0 - a_2, \end{aligned} \tag{9}$$

$\tilde{a}_0$, $\tilde{a}_1$, $\tilde{a}_2$ defined respectively as a_2, a_1, a_0 (note the ordering) but replacing according to (6) $w_{n-2} \leftrightarrow \tilde{w}_2, w_{n-1} \leftrightarrow \tilde{w}_1, \beta \to \frac{1}{\beta}, \gamma \to \frac{\gamma}{\beta^3}$.

Here and from now on in this paper, we assume, without lost of generality, that $w_n := \tilde{w}_0$ i.e. the end-weights at the common end-point of two rational curves are equal.

We also note that in our applications $den \neq 0$. To specialize to a C^2 join in homogeneous space $\mathbb{P}^{m+1}$, we define

$$\mathbb{f} := \sum_{k=0}^n \mathbb{b}_k B_k^n(u), \quad \mathbb{b}_k := \left[\begin{smallmatrix} w_k\mathbf{b}_k \\ w_k \end{smallmatrix}\right] \in \mathbb{P}^{m+1}.$$

Corollary 1 (homogeneous parametric C^2) *The homogeneous functions $\mathbb{f}$ and $\tilde{\mathbb{f}}$ join* parametrically C^2 *if $\gamma = 0$,* (8) *and* (9) *hold and the weights satisfy*

$$w_{n-1} := h_0 w_{n-2} + h_1 w_n + h_2 \tilde{w}_2 \ , \quad \tilde{w}_1 := \tilde{h}_0 w_{n-2} + \tilde{h}_1 w_n + \tilde{h}_2 \tilde{w}_2, \tag{10}$$

where $h_0 := \frac{\beta}{2(1+\beta)}$, $h_2 := -\frac{1}{2\beta(1+\beta)}$, $\tilde{h}_0 := -\frac{\beta^2}{2(1+\beta)}$, $\tilde{h}_2 := \frac{1}{2(1+\beta)}$, *and* $h_1 := 1 - h_0 - h_2$, $\tilde{h_1} := 1 - \tilde{h_0} - \tilde{h_2}$.

Proof We check, preferably with a symbolic solver, that

$$\mathbb{b}_{n-1} = h_0 \mathbb{b}_{n-2} + h_1 \mathbb{b}_n + h_2 \tilde{\mathbb{b}}_2 \ , \quad \tilde{\mathbb{b}}_1 = \tilde{h}_0 \mathbb{b}_{n-2} + \tilde{h}_1 \mathbb{b}_n + \tilde{h}_2 \tilde{\mathbb{b}}_2. \tag{11}$$

Then the C^2 constraints hold, e.g. we see that $\mathbb{b}_n = (\beta \mathbb{b}_{n-1} + \tilde{\mathbb{b}}_1)/(1+\beta)$. $|||$

Corollary 1 formally confirms the expected but not obvious property that a parametric C^2 join in homogeneous case is a special case of the local G^2 join in affine space, defined in Lemma 1. We note that according to [BP97], the C^2 homogeneous junction defined by (10) prevents reproduction of global circle with degree less than 6. By contrast, below we will construct curves of rational degree 3, including arcs of circles.

To convert the BB-coefficients $\mathbf{b}_{i,k}$ of our construction with polynomial pieces indexed by i to a sparser set of points $\mathbf{p}_i$ analogous to spline control points, we use the following Lemma 2. The lemma reflects the fact that the combinatorial structure of the rational G^2 splines is identical to that of classical C^2 splines.

Lemma 2 (B-spline-like control points) *The lines $\overline{\mathbf{b}_{i-1,1}\mathbf{b}_{i-1,2}}$ and $\overline{\mathbf{b}_{i,1}\mathbf{b}_{i,2}}$ of a G^2 rational cubic spline intersect at the point*

$$\mathbf{p}_i := (1 - l_i)\mathbf{b}_{i-1,2} + l_i \mathbf{b}_{i-1,1} = (1 - \tilde{l}_i)\mathbf{b}_{i,1} + \tilde{l}_i \mathbf{b}_{i,2} \ , \tag{12}$$

where

$$\begin{aligned} l_i :=& -\frac{2w_{i0}w_{i-1,1}(w_{i1} + w_{i-1,2}\beta_i)\beta_i^2}{c_1\beta_i + c_2\beta_i^2 + c_3\gamma_i}, \ \tilde{l}_i := \frac{w_{i2}}{w_{i-1,1}\beta_i^2} l_i \ , \\ c_1 :=& w_{i-1,2}(6w_{i1}^2 - 2w_{i0}w_{i2} - 2w_{i0}w_{i1}) \ , \ c_3 := w_{i-1,2}w_{i0}w_{i1} \ , \\ c_2 :=& w_{i1}(6w_{i-1,2}^2 - 2w_{i0}w_{i-1,1} - 2w_{i0}w_{i-1,2}) \ . \end{aligned} \tag{13}$$

If for all segments i, $w_i = 1$ and $\gamma_i = 0$ then $l_i = -\beta_i$ and $\tilde{l}_i = -1/\beta_i$.

Special cases of Lemma 2 are easy to verify; but in full generality, it is most convenient to substitute the expressions and let a symbolic solver do the work.

4 Cubic G^2 splines

For a given a control polygon $\mathbf{p}_i$, $i = 1, \ldots, N$, we want to construct BB-coefficients $\mathbf{b}_{i,k} \in \mathbb{R}^3$, $k = 0, 1, 2, 3$ of the ith curve segment. The construction is combinatorially identical to deriving the BB-coefficients of a cubic C^2 spline from its de Boor (B-spline) control points. Specifically, the affine components $\mathbf{b}_{i,1}$, $\mathbf{b}_{i,2}$ of our rational cubic G^2 spline lie on the edge $\overline{\mathbf{p}_i\mathbf{p}_{i+1}}$ and the end-points $\mathbf{b}_{i-1,3} = \mathbf{b}_{i,0}$ lie on the line $\overline{\mathbf{b}_{i-1,2}\mathbf{b}_{i,1}}$:

$$\begin{aligned}
\mathbf{b}_{i,1} &:= (1-t_i)\mathbf{p}_i + t_i\mathbf{p}_{i+1}\ ,\ t_i := -\frac{\tilde{l}_i}{1-l_{i+1}-\tilde{l}_i}\ , \\
\mathbf{b}_{i,2} &:= \tilde{t}_i\mathbf{p}_i + (1-\tilde{t}_i)\mathbf{p}_{i+1}\ , \tilde{t}_i := -\frac{l_{i+1}}{1-l_{i+1}-\tilde{l}_i} \\
\mathbf{b}_{i,0} &:= (1-x_i)\mathbf{b}_{i-1,2} + x_i\mathbf{b}_{i,1},\ x_i := \frac{w_{i,1}}{w_{i-1,2}\beta_i + w_{i,1}}\ .
\end{aligned} \tag{14}$$

The first two assignments of (14) can be viewed as an inversion of (12). The weights $w_{i,j}$ are free to be determined and l_i and $\tilde{l}_i$ are defined by (13) of Lemma 2.

Theorem 1 (G^2 continuity) *Let f_{i-1}, f_i be rational cubic curves with control points $\mathbf{b}_{i-1,k}$, $\mathbf{b}_{i,k}$ defined by* (14)*. Then*

$$f_i'(0) = \beta_i f_{i-1}'(1)\ , \quad f_i''(0) = \beta_i^2 f_{i-1}''(1) + \gamma_i f_{i-1}'(1)\ .$$

Proof For $n = 3$ and the choice of $\mathbf{b}_{i,k}$ of (14), we verify (8). |||

Specializing (14) by setting all $\gamma_i = 0$, the expressions in (14) simplify in that

$$t_i = \frac{1}{1+\beta_i+\beta_i\beta_{i+1}}\ ,\ \tilde{t}_i = \frac{\beta_i\beta_{i+1}}{1+\beta_i+\beta_i\beta_{i+1}}\ ,\ x_i = \frac{1}{1+\beta_i}.$$

Corollary 1 with $n = 3$ confirms that the rational cubic G^2 splines defined by (14) are a superset of the (homogeneous) cubic non-uniform C^2 splines. The additional complexity, hidden in (13), of the formulas (14) over cubic non-uniform C^2 splines in BB-form buys us the important reproduction property as we see next.

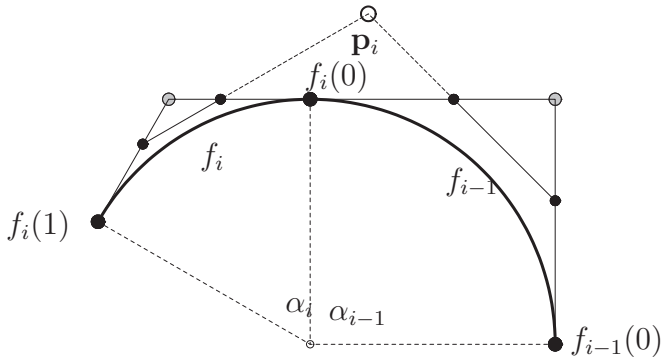

Figure 3: **Rational degree 3 representation of two adjacent arcs of a circle.** The middle coefficients of the quadratic pieces are shown as grey disks and the inner BB-coefficients $\mathbf{b}_{i-1,1}$, $\mathbf{b}_{i-1,2}$, $\mathbf{b}_{i,1}$ and $\mathbf{b}_{i,2}$ as black disks. The weights are $w_{i0} = w_{i3} = 1$, $w_{i1} = w_{i2} = \frac{1}{3} + \frac{2}{3}\cos\frac{\alpha_i}{2}$.

5 Inclusion of a rational cubic curve piece into a G^2 spline

First, we consider a general cubic curve $\mathbf{c}(u)$. Let $\mathbb{c}$ be the *homogeneous* representation of $\mathbf{c}$ and fix an increasing sequence of $u_i \in \mathbb{R}$, for example $u_i \in [0, 1]$. We can partition $\mathbb{c}$ into pieces on non-empty intervals $[u_i..u_{i+1}]$ and with G^2 parameters

$$\mathbb{f}_i(u) := \mathbb{c}(u_i(1-u) + u_{i+1}u), \qquad \beta_i = \frac{u_{i+1} - u_i}{u_i - u_{i-1}}, \quad \gamma_i = 0. \tag{15}$$

We convert each pieces $\mathbb{f}_i$ to BB-form on the interval $[0..1]$. The definition of β_i and γ_i by (15) holds for both the homogeneous representation $\mathbb{f}_i$ and the rational affine representation f_i. Spline control points $\mathbf{p}_i$ of f_i can be calculated according to (12).

Polynomial cubics and rational quadratics Next, we consider a subset of the rational cubics for which the inclusion formulas are particularly easy to write out and that are likely the most relevant cases in practice. These are polynomial cubic segments and segments $f_i(u) := f(u_i(1-u) + u_{i+1}u)$ of a rational quadratic curve f, in degree-raised representation.

Lemma 3 (reproducing rational quadratic segments) *For $i = 0, \ldots, N+1$ let f_i be a rational quadratic curve segment with* symmetric *weights $[1, w_i, 1]$.*

Let f_{i-1} and f_i be G^2-connected with parameters β_i, γ_i at $f_{i-1}(1) = f_i(0)$. For $i = 1, \ldots, N+1$, set

$$\mathbf{p}_i := y_{i0} f_{i-1}(0) + y_{i1} f_i(0) + y_{i2} f_i(1) \,, \tag{16}$$

$$y_{i0} := -\frac{2\beta_i^3}{(1+2w_i)D_i}, y_{i2} := -\frac{2}{(1+2w_{i-1})D_i}, y_{i1} := 1 - y_{i0} - y_{i2}, \tag{17}$$

where $D_i := 4w_i\beta_i + 4w_{i-1}\beta_i^2 - 2\beta_i - 2\beta_i^2 + \gamma_i$.

Then the construction (14) *reproduces the curve segments f_i for $i = 2, \ldots, N-1$.*

Formulas (16), (17) were used to construct the control polygons in Fig. 1, 2, and 4. The weights of any rational quadratic can we brought into the form $[1, w, 1]$ required by Lemma 3 by rescaling the original weights w_{i0}, w_{i1}, w_{i2} to weights $\bar{w}_{ik}$ and then re-parameterizing:

$$\begin{aligned} &\bar{w}_{ik} := \frac{w_{ik}}{w_{i0}} \,,\ k = 0, 1, 2 \,; \\ &w_{ik}^{sym} := \bar{w}_{ik}(h_i)^k,\ k = 0, 1, 2 \,; h_i := \frac{1}{\sqrt{\bar{w}_{i2}}} \,. \end{aligned} \tag{18}$$

The parameters β_i, γ_i thereby become

$$\beta_i^{sym} := h_{i-1}h_i\beta_i \,,\ \gamma_i^{sym} := 2h_{i-1}h_i(1-h_i)\beta_i - 2h_{i-1}h_i^2(1-h_{i-1})\beta_i^2 + h_{i-1}h_i^2\gamma_i.$$

For *polynomial cubic* pieces, (16) and (17) also apply, with $w_{i-1} = w_i = 1$; and β_i and γ_i are defined by (15) so that y_{i0} and y_{i2} simplify to

$$y_{i0} := -\frac{\beta_i^2}{3(1+\beta_i)}, \quad y_{i2} := -\frac{1}{3(1+\beta_i)\beta_i}. \tag{19}$$

Circular arcs Adjacent arcs of a circle, with opening angles α_{i-1} and α_i respectively as in Fig. 3, are G^∞-connected. In particular,

$$\beta_i = \frac{\sin\frac{\alpha_i}{2}}{\sin\frac{\alpha_{i-1}}{2}} = \frac{|f_{i-1}(1)f_i(1)|}{|f_{i-1}(0)f_i(0)|} \qquad \gamma_i = 2\beta_i(\tan\frac{\alpha_{i-1}}{4} + \tan\frac{\alpha_i}{4})\sin\frac{\alpha_i}{2}, \tag{20}$$

The formula for β_i exposes the fact that the arcs of a circle are parameterized by chord length [Far06]. By affine transformation, the circle construction applies to ellipses. Finally, we specialize (14) to formulas ($14_\circ$) for equi-angular arcs.

Corollary 2 (equi-angular circle arcs) *For a sequence of circle arcs with equal opening angle* $\alpha := 2\pi/m$*,*

$$\beta_i = 1,\ \gamma_i = 4(1-\cos\frac{\alpha}{2}),\ x_i = \frac{1}{2}\ ,\ t_i = \tilde{t}_i = \frac{1}{2+\cos\frac{\alpha}{2}}\ ; \qquad (14_\circ)$$

and if the control points $\mathbf{p}_i$ *form a regular* m*-gon with circumscribed circle of radius*

$$\frac{2+\cos\frac{\alpha}{2}}{\cos\frac{\alpha}{2}\left(1+2\cos\frac{\alpha}{2}\right)}\sigma\ ,$$

then a spline curve reproduces a circle of radius σ*.*

In summary, this section showed how to convert conic arcs and how to include them and other cubic curve segments into the spline of the form defined in Section 4.

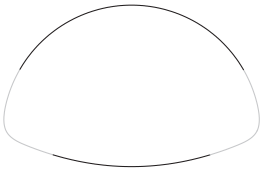

(a) circle & parabola

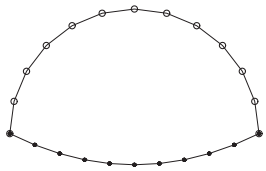

(b) control polygon

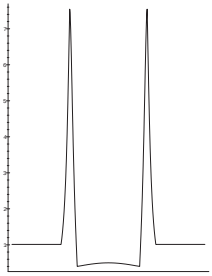

(c) curvature of G^2 spline

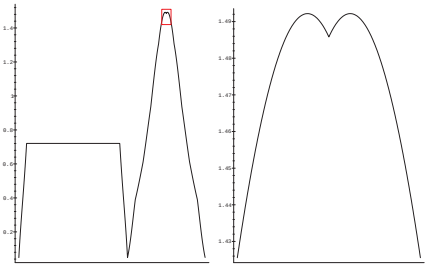

(d) [Rom09] circle-reproducing

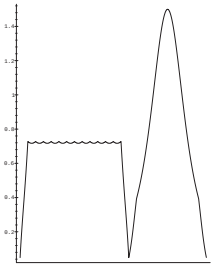

(e) parabola-repro

Figure 4: Comparison: **Reproducing multiple conics.** (a) Cubic G^2 spline reproducing a circle segment and a parabola segment (thick segments). (b) The control points are marked "o" for the circle and "•" for the parabola. (c) Curvature (flat for the circle, rounded for the parabola) of the G^2 spline. A visually alike uniform non-stationary subdivision curve has incorrect curvature either for (d) the parabola (note the dip in magnification), or (e) for the circle (note the oscillation).

6 Comparison to non-stationary circle-preserving subdivision schemes

To highlight the importance of non-uniformity, we compare the new G^2 rational cubic splines with two curve construction schemes that can reproduce circles but are based on uniform knot spacing. The first is a uniform non-stationary C^2 subdivision [Rom09] that, at first sight, creates very similar curves to the spline. The second, [MWW01], is also a non-stationary subdivision scheme, but can model more than one basic shape.

The subdivision scheme [Rom09] is defined by Laurent polynomial $\frac{1}{2}(z+1)^2\frac{z^2+2v^{k+1}z+1}{2(v^{k+1}+1)}$, i.e. new points $\mathbf{p}_i^{k+1}$ are derived from older ones at step k by

$$\begin{aligned}\mathbf{p}_{2i+1}^{k+1} :=& \frac{1}{2}\mathbf{p}_i^k + \frac{1}{2}\mathbf{p}_{i+1}^k \quad v^{k+1} := \sqrt{(1+v^k)/2},\\ \mathbf{p}_{2i}^{k+1} :=& \frac{1}{4(1+v^{k+1})}\mathbf{p}_{i-1}^k + \frac{1+2v^{k+1}}{2(1+v^{k+1})}\mathbf{p}_{i-1}^k + \frac{1}{4(1+v^{k+1})}\mathbf{p}_{i+1}^k\,.\end{aligned}$$

If the input is a regular m-gon and $v^0 := \cos(2\pi/m)$, then the limit curve is a circle.

The point of comparing to the subdivision scheme in Fig. 4 is that schemes like [Rom09] only reproduce one type of primitive in a composite curve. Based on the choice of v^0, either the circle or the parabola is correctly replicated but not both. Other subdivision schemes, e.g. [DS09], behave similarly. By contrast, G^2 splines are capable of preserving shapes locally: Fig. 5 shows inclusion of both a circle segment and an ellipse segment into one G^2 spline curve.

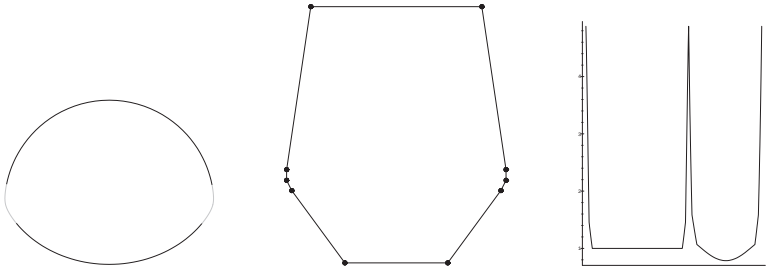

(a) circle & ellipse (b) control polygon (c) curvature

Figure 5: G^2 spline **reproducing multiple conics.**

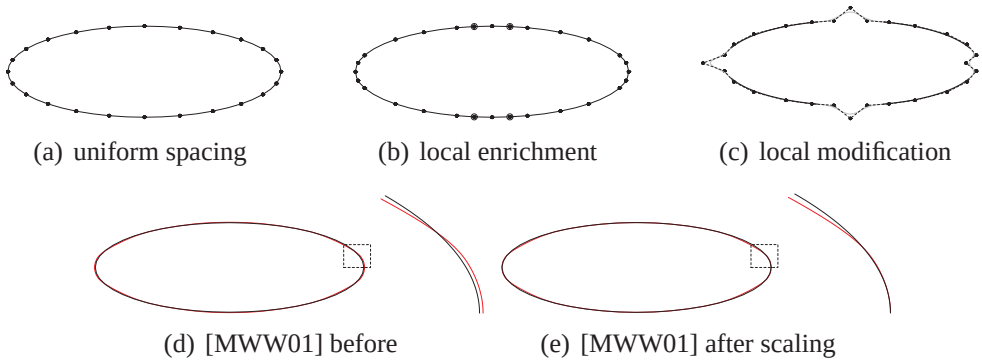

(a) uniform spacing (b) local enrichment (c) local modification

(d) [MWW01] before (e) [MWW01] after scaling

Figure 6: **Design modification** with the G^2 rational cubic spline (a,b,c). (b) exactly reproduces the ellipse with non-uniform segments. (d) and (e) show two failed attempts at reproducing the ellipse with non-uniform segments using [MWW01] illustrating that it cannot be used for the localized modification.

Second, we compare to [MWW01] which is one of the few non-stationary subdivision schemes that can model more than one basic shape in one spline. Its simplest version with uniform parameter $v_i^0 = const$, called tension in [MWW01], is shared with [Rom09] and allows only reproduction of one primitive as in Fig. 4. But the generalization by varying the tension allows reproducing all conics in a single curve. The point of comparison here is that [MWW01] is based on uniform knot spacing. Fig. 6 demonstrates that standard tasks, like local modification, become awkward when non-uniformity is excluded. In (a) a circle has been uniformly sampled and scaled to form an ellipse. These samples are the starting point of a design modification. First, in (b), the samples are enriched (larger markers) and non-uniformly redistributed (four points in the high curvature parts of the ellipse, *left* and *right*). The G^2 rational cubic spline construction can still reproduce the ellipse also with this non-uniform spacing of control. Fig. 6(c) shows a local modification so that thick segments of the rational cubic spline remain on the ellipse. For comparison, we try, in (d,e), to achieve (b) with the algorithm of [MWW01]. For a regular polygon on the unit circle with opening angle α, [MWW01] produces a circle of radius $\frac{\sin(\alpha)}{\alpha}$. If the designer's spacing of samples for perturbation is to be honored in the control polygon, the control points' distance to the circle center must be scaled differently for the low curvature and for the high curvature parts of the ellipse. In (d) the control polygon is uniformly scaled to come close to the overall ellipse. In (e) the polygon is scaled to match the *right* ellipse segment exactly. In neither case can the ellipse be reproduced

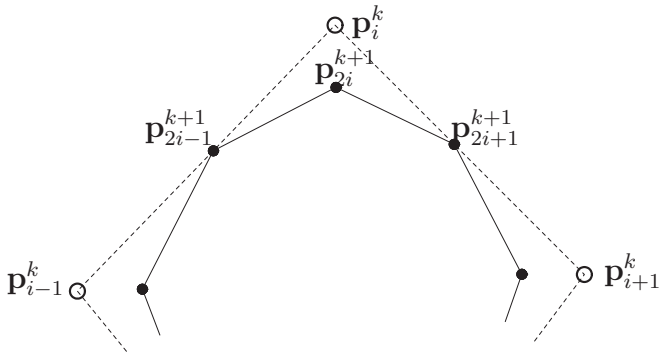

Figure 7: Refinement of a C^2 spline control net.

while honoring the local choice of control point density. The magnifications of the boxed regions show the exact ellipse in *black* and the result of [MWW01] in *red*. Clearly, in the transition, the reproduction is lost.

7 Subdivision from rational G^2 cubics

To complete the exposition of rational G^2 cubics, we derive an algorithm for control point refinement. This algorithm is analogous to the refinement of a non-uniform cubic C^2 B-spline curve, illustrated in Fig. 7. The next paragraph gives explicit formulas.

Non-uniform subdivision of C^2 splines Given the knot sequence $\{t_i\}$ and control polygon $\{\mathbf{p}_i^k\}$, we set $\bar{t}_{2i} := t_i$ and insert new knots at $\bar{t}_{2i+1} := (1-e_i)t_i + e_i t_{i+1}$, $0 < e_i < 1$. Then the refined polygon $\{\mathbf{p}_i^{k+1}\}$ of a C^2 spline with control points $\mathbf{p}_i^k$ is

$$\mathbf{p}_{2i+1}^{k+1} := (1-x_i)\mathbf{p}_i^k + x_i\mathbf{p}_{i+1}^k \,, \tag{21}$$

$$\mathbf{p}_{2i}^{k+1} := y_i\mathbf{p}_{2i-i}^{k+1} + (1-y_i-z_i)\mathbf{p}_i^k + z_i\mathbf{p}_{2i+i}^{k+1} \tag{22}$$

$$\beta_i := \frac{t_{i+1}-t_i}{t_i-t_{i-1}}, \qquad x_i := \frac{1+e_i\beta_i}{1+\beta_i+\beta_i\beta_{i+1}} \,,\; y_i := \frac{\beta_i(1-e_i)}{1+\beta_i} \,,\; z_i := \frac{e_{i-1}}{1+\beta_i}.$$

For the next refinement step $\beta_{2i}^{new} := \frac{e_i}{1-e_{i-1}}\beta_i$, $\beta_{2i+1}^{new} := \frac{1-e_i}{e_i}$.

Subdivision of G^2 splines To derive an analogous refinement of G^2 splines, there are two strategies. The first is to refine the control polygon formed by

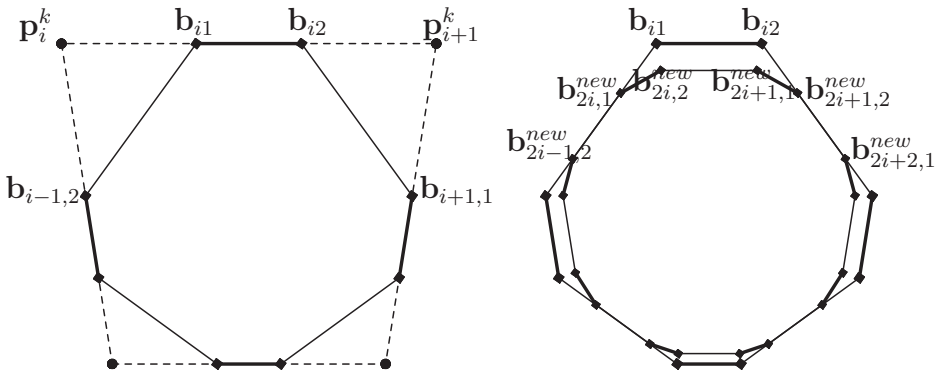

Figure 8: (*left*) Conversion (14) to BB-form and (*right*) subdivision in terms of BB-coefficients.

points $\mathbf{p}_i^k$ directly – this leads to complex formulas relegated to the technical report [KP11] . The second, and our preferred approach, refines the control polygon consisting of the interior BB-coefficients $\mathbf{b}_{i1}$, $\mathbf{b}_{i2}$, the weights and the G^2 parameters β_i, as in Fig. 8. This is an atypical approach to subdivision since the sets $\{\mathbf{b}_{i1}\}$ and $\{\mathbf{b}_{i2}\}$ are dependent; but it leads to comparatively much shorter formulas. The parameters γ_i are only needed if we want to recover refined spline coefficients $\mathbf{p}_i^k$.

Consider a sequence $\{e_i\}$, $0 < e_i < 1$, e.g. $e_i = 1/2$ for midpoint refinement. Parameters w_{i1}, w_{i2} are originally assigned to the edge $\mathbf{p}_i^k\mathbf{p}_{i+1}^k$, and parameters $W_i := w_{i-1,3} = w_{i,0}$, β_i, γ_i are assigned to the point $\mathbf{p}_i^k$. We initially apply (14) to obtain the (homogeneous) BB-control points of each rational cubic.

To obtain new control points and weights, we split the homogeneous BB-form of the ith segment at e_i by de Casteljau's algorithm. Explicitly, the refinement rules $\{\mathbf{b}_i\} \to \{\mathbf{b}_j^{new}\}$ are

$$\mathbf{b}_{2i,1}^{new} := d_{10}^i \mathbf{b}_{i-1,2} + d_{11}^i \mathbf{b}_{i1}\ , \quad \mathbf{b}_{2i,2}^{new} := d_{20}^i \mathbf{b}_{i-1,2} + d_{21}^i \mathbf{b}_{i1} + d_{22}^i \mathbf{b}_{i2}, \tag{23}$$

$$\mathbf{b}_{2i+1,1}^{new} := \tilde{d}_{10}^i \mathbf{b}_{i+1,1} + \tilde{d}_{11}^i \mathbf{b}_{i2} + \tilde{d}_{12}^i \mathbf{b}_{i1}, \quad \mathbf{b}_{2i+1,2}^{new} := \tilde{d}_{20}^i \mathbf{b}_{i+1,1} + \tilde{d}_{21}^i \mathbf{b}_{i2} \tag{24}$$

where $\tilde{d}_{10}^i$, $\tilde{d}_{11}^i$, $\tilde{d}_{12}^i, \tilde{d}_{20}^i, \tilde{d}_{21}^i$ are obtained from d_{20}^i, d_{21}^i, d_{22}^i, d_{10}^i, d_{11}^i by replacing the weights $w_{i-1,2} \to w_{i+1,1}$, $W_i \to W_{i+1}$, $w_{i1} \leftrightarrow w_{i2}$, $\beta_i \to \frac{1}{\beta_{i+1}}$, $e_i \to 1 - e_i$,

$w^{new}_{2i,1} \to w^{new}_{2i+1,2}$, $w^{new}_{2i,2} \to w^{new}_{2i+1,1}$ and

$$d^i_{10} := \frac{(1-e_i)w_{i-1,2}W_i\beta_i}{(w_{i1}+w_{i-1,2}\beta_i)w^{new}_{2i,1}}\ ,\ d^i_{11} := 1 - d^i_{10}\ ,$$
$$d^i_{20} := \frac{(1-e_i)^2w_{i-1,2}W_i\beta_i}{(w_{i1}+w_{i-1,2}\beta_i)w^{new}_{2i,2}}\ ,\ d^i_{22} := \frac{e_i^2 w_{i,2}}{w^{new}_{2i,2}}\ ,\ d^i_{21} := 1 - d^i_{00} - d^i_{20}\ .$$

Then, from (7), the new constants of G^2 continuity are

$$\beta^{new}_{2i} := \frac{e_i}{1-e_{i-1}}\beta_i\ ,\ \gamma^{new}_{2i} := \frac{e_i^2}{1-e_{i-1}}\gamma_i\ , \beta^{new}_{2i+1} := \frac{1-e_i}{e_i}\ ,\ \gamma^{new}_{2i+1} := 0. \quad (25)$$

By a slight adjustment (see the technical report [KP11]), formulas (23) and (24) yield a localized subdivision.

While structurally simple, the explicit formulas (23) and (24) for subdivision are still more complex than the formulas (13) and (14) for splines. That is, while subdivision is often viewed as 'simplifying the math', the opposite seems to be the case when trying to reproduce prescribed shapes.

8 Quadratic reparameterization yields C^2 rational quartic splines

Some modeling applications, e.g. a motion following the curve in terms of the curve's parameterization, require parametric smoothness. In this section we replace each cubic segment with two quartic segments, such that the resulting quartic curve is parametrically C^2 and reproduces the same basic shapes as the cubic G^2 construction did. While not identical, the G^2 cubic curve and the C^2 quartic curve derived from it are near-indistinguishable both visually and in curvature plots.

By (5) no linear reparameterization of the G^2 cubic spline results in a C^2 parametrization. When searching for a suitable rational reparameterization of degree 2, we discovered a preferred map z, defined on $[0,1]$ by

$$z(u) := \frac{\nu(1-u)u + u^2}{(1-u)^2 + \nu 2(1-u)u + u^2} \qquad \nu := \frac{1+\sqrt{5+4Z}}{2(1+Z)}, \quad (26)$$

where ν is a positive root of the equation $(1+Z)x^2 - x - 1 = 0$. The following Lemma 4 establishes that we can indeed non-uniformly parameterize circles as C^2 functions with the help of z. The lemma is checked directly by expansion.

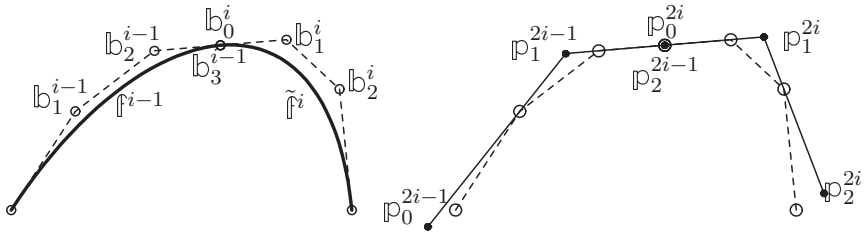

Figure 9: **Homogeneous G^2 cubics**. (*left*) Control points $\mathbb{b}_k^{i-1}$ and $\mathbb{b}_k^i$ of two adjacent G^2 cubics. (*right*) The 2-jets of the cubics at the common point $\mathbb{p}_2^{2i-1} = \mathbb{p}_0^{2i} = \mathbb{b}_3^{i-1} = \mathbb{b}_0^i$ represented by three coefficients $\mathbb{p}_\ell^{2i-1}$ and $\mathbb{p}_\ell^{2i}$ each, defined by (29).

Lemma 4 (circular arc reparameterization to C^2) *Let f, $\tilde{f}$ be adjacent circular arcs with the opening angles α, $\tilde{\alpha}$,*

$$Z := \cos(\alpha/2),\ \tilde{Z} := \cos(\tilde{\alpha}/2), \quad g(u) := f(z(u)),\ \tilde{g}(u) := \tilde{f}(\tilde{z}(u)), \tag{27}$$

then

$$\tilde{g}' = \frac{\tilde{\nu}}{\nu}\beta g'\ ,\ \tilde{g}'' = \left(\frac{\tilde{\nu}}{\nu}\beta\right)^2 g''\ , \tag{28}$$

where β is defined by formula (20)*.*

For uniform partitions with opening angle α and hence $Z := \cos\alpha/2$, our map z reduces to a map called 'zigzag' map by [BS96]. We therefore refer also to our reparameterization as (non-uniform) zigzag map.

We derive C^2 connected quartics from our rational G^2 cubics as follows. Consider two cubic splines f^{i-1}, f^i that join G^2 with $(f^i)' = \beta_i (f^{i-1})'$, $(f^i)'' = \beta_i^2 (f^{i-1})'' + \gamma_i (f^{i-1})'$. First, as illustrated in Fig. 10, *top,left*, we collect at their meeting point their 2-jets represented by triples of homogeneous BB control points $\mathbb{b}_k^\ell$, $\ell \in \{i-1, i\}$. We write the 2-jets as if they came from two quadratic functions $\mathbb{p}^j$, $j \in \{2i-1, 2i\}$ with coefficients $\mathbb{p}_k^j$ (cf. Fig. 9),

$$\begin{aligned} \mathbb{p}_2^{2i-1} :=& \mathbb{b}_3^{i-1}\ ,\ \mathbb{p}_1^{2i-1} := -\frac{1}{2}\mathbb{b}_3^{i-1} + \frac{3}{2}\mathbb{b}_2^{i-1}\ ,\ \mathbb{p}_0^{2i-1} := \mathbb{b}_3^{i-1} - 3\mathbb{b}_2^{i-1} + 3\mathbb{b}_1^{i-1}\ , \\ \mathbb{p}_0^{2i} :=& \mathbb{b}_0^i\ ,\ \mathbb{p}_1^{2i} := -\frac{1}{2}\mathbb{b}_0^i + \frac{3}{2}\mathbb{b}_1^i\ ,\ \mathbb{p}_2^{2i} := \mathbb{b}_0^i - 3\mathbb{b}_1^i + 3\mathbb{b}_2^i\ . \end{aligned} \tag{29}$$

We compose the $\mathbb{p}^j$ with a zigzag map each, extract once more their 2-jets and scale them by 1/2 to obtain their representation as control points $\mathbb{q}_k^{2i-1}$, $k = 2, 3, 4$ of the right degree 4 curve piece $\mathbb{q}^{2i-1}$ derived from f^{i-1} and $\mathbb{q}_k^{2i}$, $k = 0, 1, 2$ of the

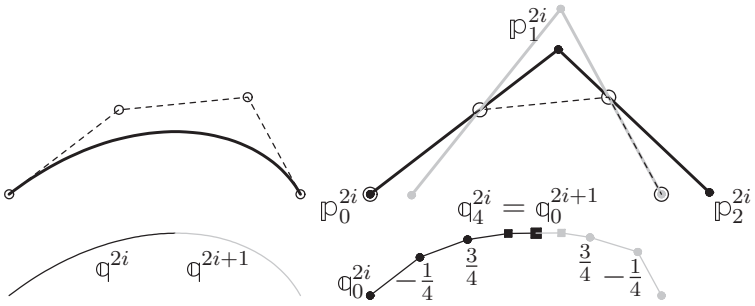

Figure 10: **Degree 4 splines derived from Hermite data.** (*top left*) A cubic G^2 spline and (*top right*) its two 2-jets at the endpoints (cf. Fig. 9). (*bottom left*) The final of two quartic curve pieces and (*bottom right*) their control points.

left degree 4 curve piece $\mathbb{q}^{2i}$ derived from f^i (cf. Fig. 10). The scaling of 2-jets by 1/2 may be viewed as subdividing at the midpoint the composition $\mathbb{p}^j \circ z^j$. Direct calculation shows the resulting jets are C^2 connected if and only if

$$\beta_i^2 Z^{2i-1} + \beta_i Z^{2i} - \beta_i - \beta_i^2 + \frac{1}{2}\gamma_i = 0. \tag{30}$$

With $w_{j,k}$ the weight coordinate of $\mathbb{p}_k^j$, we pick the symmetric choice

$$Z_0^{2i-1} := \frac{w_{2i-1,1}}{w_{2i-1,2}},\ Z_0^{2i} \text{ from (30)}, \quad Z_1^{2i} := \frac{w_{2i,1}}{w_{2i,0}},\ Z_1^{2i-1} \text{ from (30)}, \tag{31}$$

$$Z^{2i-1} := (Z_0^{2i-1} + Z_1^{2i-1})/2, \qquad Z^{2i} := (Z_0^{2i} + Z_1^{2i})/2. \tag{32}$$

Now consider the 2-jets at either endpoint of one segment as illustrated in Fig. 10, *top*. The black control polygon $\mathbb{p}_0^{2i}$, $\mathbb{p}_1^{2i}$, $\mathbb{p}_2^{2i}$ belongs to the left endpoint. The unlabeled gray control polygon is formed by points $\mathbb{p}_k^{2i+1}$ and belongs to the right endpoint. Together they define the two abutting homogeneous quartic curve segments $\mathbb{q}^{2i}$ and $\mathbb{q}^{2i+1}$ shown in Fig. 10, *bottom,left*, whose coefficients $\mathbb{q}_3^{2i}$ and $\mathbb{q}_4^{2i} = \mathbb{q}_0^{2i+1}$ and $\mathbb{q}_1^{2i+1}$ (black and gray squares in Fig. 10, *bottom,right*) are determined so that $\mathbb{q}^{2i}$ and $\mathbb{q}^{2i+1}$ join C^3. Fig. 10, *bottom,right*, gives the weights for computing the common endpoint $\mathbb{q}_4^{2i} = \mathbb{q}_0^{2i+1}$ (the largest black square). All joins are now at least C^2. Since the subquartics $\mathbb{q}^{2i}$ and $\mathbb{q}^{2i+1}$ coincide with the pieces of one quartic split if the data are from one quartic, any zigzag-reparametrized quadratic curve segment is reproduced by the two subquartics.

9 Cubic reparameterization yields circle-reproducing C^2 splines in homogeneous space

The elegant method of [BP97] can construct circles as uniform C^2 sextic splines in homogeneous space. However, uniform splines are restrictive when combining different basic shapes in design. We therefore present a rational C^2 cubic re-parameterization that allows for a generalization of [BP97] using three pieces per arc. We do not give the technical details of this curve construction since it retraces the steps of the previous section, i.e. deriving 2-jets, reparameterizing, scaling the jets and joining the pieces C^2. Instead we focus on the key points: the piecewise degree 3 reparameterization r, and the smoothness at the original junctions between arcs.

We consider a circular arc $\mathbb{f}^0$ and its two neighbors $\mathbb{f}^{-1}$ and $\mathbb{f}^1$ with corresponding opening angles α_{-1}, α_0, α_1. We reparameterize $\mathbb{f}^0$ by the three segments $r^j : [0,1] \to \mathbb{R}$ of the rational cubic reparameterization. The homogeneous control points ρ_k^j, $k = 0 \ldots 3$, $j = 0, 1, 2$ of r^j are defined as follows (cf. Fig. 11).

- We set $\tau_\ell := \tan \frac{\alpha_\ell}{4}, \quad \eta := 7\tau_0^3\tau_1 + 7\tau_0\tau_1 + 5\tau_0^2 + 2\tau_0^2\tau_1^2 + 3\,,$

$$d := \frac{(1+\tau_0^2)(3\tau_0\tau_1+1)}{\eta}, \quad \nu := \frac{(1+\tau_0\tau_1)\eta}{(1+\tau_0^2)(3\tau_0\tau_1+1)(\tau_0\tau_1+3)}.$$

- We define a rational cubic map $h^1(u) : [0,1] \to \mathbb{R}$ by homogeneous control points

$$h_0^1 := \left[\begin{smallmatrix}0\\1\end{smallmatrix}\right],\ h_1^1 := \left[\begin{smallmatrix}\nu d\\ \nu\end{smallmatrix}\right],\ h_2^1 := \left[\begin{smallmatrix}\nu(1-d)\\ \nu\end{smallmatrix}\right],\ h_3^1 := \left[\begin{smallmatrix}1\\1\end{smallmatrix}\right],$$

  and a second, symmetric one, $h^0(u)$, by replacing in h^1: $\tau_1 \to \tau_{-1}$.

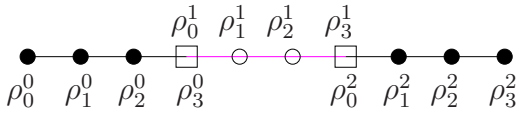

Figure 11: Coefficients of the **rational cubic reparameterization**.

- We obtain the left piece of our reparameterization as $r^0(u) := h^0(u/3)$ and the right as $r^2(u) := h^1(2/3 + u/3)$ with corresponding homogeneous control points ρ_k^0, ρ_k^2.

- We overwrite the end points ρ_3^0 and ρ_0^2 and set the remaining coefficients of the middle piece so that the three pieces join C^2:

$$\rho_3^0 := -\frac{1}{3}\rho_1^0 + \frac{7}{6}\rho_2^0 + \frac{1}{3}\rho_1^2 - \frac{1}{6}\rho_2^2\,, \quad \rho_0^2 := -\frac{1}{6}\rho_1^0 + \frac{1}{3}\rho_2^0 + \frac{7}{6}\rho_1^2 - \frac{1}{3}\rho_2^2, \tag{33}$$

$$\rho_0^1 := \rho_3^0, \quad \rho_1^1 := 2\rho_3^0 - \rho_2^0, \quad \rho_2^1 := 2\rho_0^2 - \rho_1^2, \quad \rho_3^1 := \rho_0^2. \tag{34}$$

Formulas (33) and (34) enable the C^2 construction internal to the ternary-split arcs which is analogous to Section 8. The following lemma establishes C^2 smoothness just between adjacent rational quadratic arcs reparameterized by their angle-dependent rational cubic maps r^j.

Lemma 5 (homogeneous C^2 reparameterization for circles) *Let $\mathbb{f}$ have opening angle α and $\overline{\mathbb{f}}$ be an adjacent circle piece with opening angle $\overline{\alpha}$. Define*

$$\overline{r}^j \text{ by replacing in } r^j : \tau_{-1} \to \tau_0, \tau_0 \to \tau_1, \tau_1 \to \tau_2. \tag{35}$$

Then the pieces $\mathbb{f}(r^2)$ and $\overline{\mathbb{f}}(\overline{r}^0)$ of the circular sextic defined by cubic reparameterization are C^2-connected in homogeneous space with $\beta = \frac{\sin\frac{\overline{\alpha}}{2}}{\sin\frac{\alpha}{2}}$.

If $\alpha_{-1} = \alpha_0 = \alpha_1$ then the pieces r^j of the reparameterization become a single cubic that agrees with the reparameterization of [BP97].

10 Discussion and Conclusion

Since the constructions are purely geometric, no basis functions were needed. However, analogous to C^2 cubic splines, we can derive basis function from the construction. As sketched in Fig. 12 *left*, each control point affects four curve segments. Setting all but one control points to zero, we get piecewise G^2 rational cubic function whose specific shape depends on the reproduction selected.

The C^2 construction in Section 8 can alternatively be modified to only use one quartic instead of two for each piece of the G^2 cubic. While such a construction usually works well, it leads to small oscillations where a line segment transitions into a non-linear cubic curve.

We constructed rational splines of higher degree and higher continuity (G^3, G^4, G^5) patterned after B-splines, but only in the uniform case. As this paper argued earlier, uniform constructions are too restrictive for practical design applications. However, we stopped developing explicit algorithms for the non-uniform

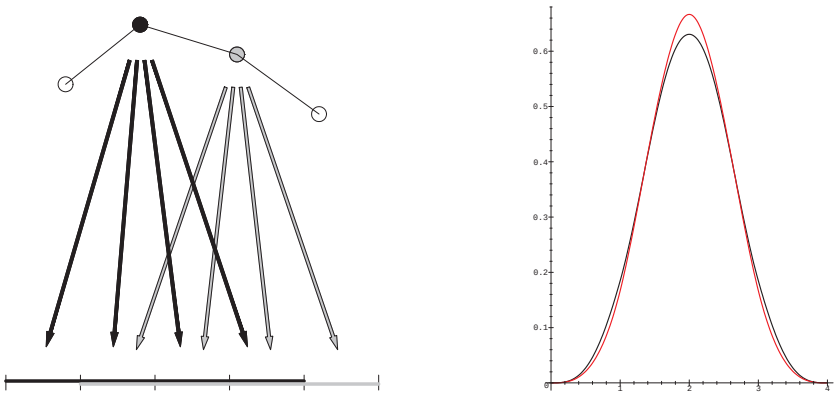

Figure 12: **Basis functions for rational cubic splines.** (*left*) Schema of influence. (*right*) Basis functions. The black curve is a uniform G^2 cubic spline that reproduces a circle via arcs with an opening angle $\pi/2$; the red curve is a uniform polynomial cubic C^2 spline.

case since the rules turned out to be too complex for practical use; and the motivation, the reproduction of exact shapes beyond conics and the need for smoothness beyond curvature continuity, is not as compelling as for G^2 cubics. By contrast, the step from G^1-connected quadratics to G^2 cubics visibly improves shape and does not yield overly complex rules.

Summary In summary, we exhibited formulas (14) for rational G^2 cubics capable of representing multiple rational quadratics and cubics in one spline. We leveraged geometric continuity in place of non-uniform knots and based the derivation as well as a subdivision scheme on the BB-form – although we could obtain B-spline-like points from this. The formulas are only moderately more complicated than those of the well-known C^2 cubic spline. The resulting curves compare well both with homogeneous C^2 splines of much higher degree and with current non-stationary subdivision schemes. Finally, we exhibited a quadratic and a cubic reparameterization to turn the rational G^2 cubic into parametrically C^2 piecewise rational curves, respectively into homogeneous C^2 splines.

Acknowledgments.

Work supported in part by NSF Grant CCF-0728797. We thank the referees for their constructive comments to improve the presentation.

References

[ADS10] Ursula H. Augsdörfer, Neil A. Dodgson, and Malcolm A. Sabin. Variations on the four-point subdivision scheme. *Computer Aided Geometric Design*, 27(1):78–95, 2010.

[Boe87] Wolfgang Boehm. Rational geometric splines. *Computer Aided Geometric Design*, 4(1-2):67–77, July 1987.

[BP97] Claudia Bangert and Hartmut Prautzsch. Circle and sphere as rational splines. *Neural, Parallel and Scientific Computations*, (5):153–162, 1997.

[BS96] Carole Blanc and Christophe Schlick. Accurate parametrization of conics by NURBS. *IEEE Computer Graphics & Applications*, 16(6):64–71, November 1996.

[DS09] S. Daniel and P. Shunmugaraj. An approximating C^2 non-stationary subdivision scheme. *Computer Aided Geometric Design*, 26:810–821, 2009.

[Far06] Gerald E. Farin. Rational quadratic circles are parametrized by chord length. *Computer Aided Geometric Design*, 23(9):722–724, 2006.

[GB88] Ronald N. Goldman and Brian A. Barsky. Beta continuity and its application to rational beta-splines. Technical Report CSD-88-442, University of California, Berkeley, August 1988.

[HB89] Michael E. Hohmeyer and Brian A. Barsky. Rational continuity: Parametric, geometric, and frenet frame continuity of rational curves. *ACM Transactions on Graphics*, 8(4):335–359, October 1989.

[Joe90] Barry Joe. Quartic beta-splines. *ACM Transactions on Graphics*, 9(3):301–337, 1990.

[KP11] Kęstutis Karčiauskas and Jörg Peters. Rational G^2 splines. Technical Report UF-CISE-2011-513, University of Florida, January 2011.

[MB89] Dinesh Manocha and Brian A Barsky. Basis functions for rational continuity. In *CG International '90*, pages 521–541, 1989.

[MB91] Dinesh Manocha and Brian A. Barsky. Varying the shape parameters of rational continuity. In *Curves and surfaces (Chamonix-Mont-Blanc, 1990)*, pages 307–313. Academic Press, Boston, MA, 1991.

[MWW01] Géraldine Morin, Joe D. Warren, and Henrik Weimer. A subdivision scheme for surfaces of revolution. *Computer Aided Geometric Design*, 18(5):483–502, 2001.

[Rom09] L. Romani. From approximating subdivision schemes for exponential splines to high-performance interpolating algorithms. *Journal of Computational and Applied Mathematics*, 224(1):383 – 396, 2009.